TITLE: Physical modeling the formation of roof collapse zones in Vorkuta coal mines

AUTHORS: Boris Yu ZUEV,Ruslan S ISTOMIN,Stanislav V KOVSHOV,Vyacheslav M KITSIS

PAGES: 225-234

ORIGINAL PDF URL: https://dergipark.org.tr/tr/download/article-file/808430

Bulletin of the Mineral Research and Exploration

http://bulletin.mta.gov.tr

Physical modeling the formation of roof collapse zones in Vorkuta coal mines

Boris Yu ZUEV[a] , Ruslan S. ISTOMIN[b] , Stanislav V. KOVSHOV[a*] and Vyacheslav M. KITSIS[b]

[a]*Saint Petersburg Mining University, 21st Line, St Petersburg 199106, Russia*
[b]*National Research Mordovia State University 68/1 Bolshevistskaya St., Saransk, 430005, Russia*

Research Article

ABSTRACT

Collapse of the roof during mining is a constant threat to the lives of miners and equipment performance. To predict it, different numerical and physical approaches are used. Physical modeling of the massif region from -951 m to -841 m using equivalent materials were undertaken in this investigation. Various options for mining the Vorkuta coal deposit were considered: mining only the upper industrial seam, mining the lower coal seam as a protective layer to the upper one, and assessing the impact on the collapse zone of the complex structure of the upper coal seam roof while maintaining an upward order of mining. The main results were as follows: calculated collapse zone is approximately 30% larger than theoretical; collapse zone decreased when using mining with lower protective coal seam; the largest collapse zone was observed when pinching the rocks in upward mining order. Therefore, the research has shown the need to adjust the project for a larger methane yield. Further large-scale modeling is needed for understanding the characteristics of the collapse zone.

1. Introduction

The collapse of the roof in the conditions of coal mines is a complex gas-dynamic and geomechanical phenomenon, accompanied by the release of a large amount of methane (Kazanin and Sidorenko, 2017*a*; Sidorenko et al., 2018). At this time, the most common emergencies occur during the underground mining of minerals, the most severe of which is accompanied by human and infrastructural losses (Gridina and Andreev, 2016). Most often, the collapse occurs in the intervals between mine working and support, or between the support racks, if the technological mode of their installation is not observed (Sidorenko and Sishchuk, 2016). The collapse mechanism is a complex process. As the face moves, the roof hangs behind the bottom, which leads to a gradual stretching of the coal seam

and the formation of microcracks in the rock mass, gradually saturated with methane. At the moment of reaching the ultimate strength, the destruction begins with the subsequent splitting of the massif into micro blocks, and the roof caving occurs, under the influence of rock pressure with the formation of methane accumulations in the goaf, as well as in the face due to the unloading of the formation (Kazanin et al., 2017). The cracks formed in the zone of collapse beyond the stope, penetrate the roof for a considerable distance and due to them the flow of methane into the goaf from the accompanying beds increases. In subsequent collapses, this methane enters the face and increases in concentration, which is fixed by the aerogas control system and it stops the equipment in an emergency (Kazanin and Sidorenko, 2017*b*).

Mathematical and computer modeling are widely used in the mining industry (Gao et al., 2014; Sidorov et al., 2018; Grigoriev et al., 2019). In order to predict the formation of zones of collapse, various methods of physical and computer modeling are applied (Andreev and Gridina, 2016; Sidorenko et al., 2019). It is also used computer modeling, e.g. 3D subsurface modeling for prediction and visualization of ore extraction in an optimal way (Akıska and Akıska, 2018). Finite Element Method as a variation of numerical analyses was successfully used for characterization of rock masses in the tunnel (Kanik et al., 2015). Nevertheless, both empirical and computational analyses should be combined with each other for the best tunnel project design (Kaya et al., 2011). Therefore, the virtue of physical modeling in its visibility. One of the main directions of physical modeling of such processes is modeling on equivalent materials (Wang et al., 2017; Gao et al., 2019; Pan et al., 2019). Having its drawbacks, such as labor and material intensity, the possibility of developing a small number of options, this method is suitable for obtaining data on the state of the simulated rock mass in a destroyed area, with the stochastic nature of the development of destruction processes. Physical modeling practices also help to verify technics for hard roof treatment (Bai et al., 2017). Physical field tests are used to find changes in roof bolt loading, roof separation and roadway deformation (Wang et al., 2019*b*). Physical modeling also can be applied for estimation of the backfilling strip mining method usage against surface collapse (Wang et al., 2019*a*). Acoustic emission can be used for monitoring rock bursts caused by hard roof failure (Li et al., 2015). Therefore, physical modeling was applied in simulation the processes of formation of the collapse zone for the Vorkuta coal deposit (Cherkai and Gridina, 2017). This method ensures the reproduction of the physicomechanical properties and structure of the rock mass, which plays a key role in solving all simulated geomechanical processes (Kang et al., 2018).

2. Materials and Methods

The relationship between full-scale materials and equivalent materials (EM) is established through linear scales α_l and the ratio of the weights α_γ.

For a detailed reproduction of the structure of the rock mass, the geometric scale of models no. 1, 2, and 3, $\alpha_l = 1: 100$ was chosen. Considering the parameters of the mass, strength and deformation criteria - the main design parameters of the EM in models no. 1, 2, and 3, were determined (Table 1).

For further research, EM with a filler of fine-grained quartz sand (0.1-0.6 mm) and a binder based on DEG-1 and ED-20 resin was chosen as base materials. The main idea of selecting the required formulation of EM was to vary the percentage of the binder for ensuring the required strength parameters of EM in accordance with table 1.

EM manufacturing technology and testing consisted of 9 steps:

1. Evaluation of the particle size distribution of the filler.

2. Dosing and weighing of the filler and the binder were carried out on standard scales with an accuracy not exceeding 1-2%.

3. Mixing the mixture of filler and binder. Laying in a timbering.

4. Rolling was carried out in layers after leveling the surface of the mixture. The weight of the roller corresponded to the optimum specific load of 2.35 N/cm^2.

5. Storage for stabilizing the properties of EM. Storage time - 3 days, until full solidification.

6. Production of EM samples. The dimensions of the samples for testing on the press - 5x5x10 cm.

7. Testing the samples on the press was carried out on uniaxial compression to determine compressive strength. Comparison of obtained data with their desired values, the adjustment of the formulation. Predictive assessment of the influence of the percentage composition of the binder in accordance with the developed methodology was made.

8. The repetition of the technological cycle (steps 2-8) was carried out according to the next predictive adjustment. The cycles were ended after overlapping with the actual values of the required strength parameters.

As a result of the implementation of this technological research program, the following types

Table 1- Physical and mechanical properties in nature and model.

Stratum (m)	Layer thickness (m)	Rocks composition	Strength full-scale (Mpa)	Strength EM (Mpa)	Notice
110					
103	7	sandstone	80	0.44	
98	5	sandstone	80	0.44	
91	7	sandstone	90	0.50	
87	4	aleurolite	80	0.44	
84	3	sandstone	90	0.50	
80	4	aleurolite	60	0.33	
78	2	argillite	39	0.22	
76	2	aleurolite	55	0.31	
68	8	sandstone	90	0.50	
61	7	sandstone	97	0.54	
56	5	sandstone	96	0.53	
51	5	sandstone	85	0.47	
49	2	aleurolite	61	0.34	
47	2	sandstone	70	0.39	
44	3	aleurolite	60	0.33	
40	4	*coal*	15	0.08	productive formation H = -930 m
37	3	aleurolite	40	0.22	
33	4	sandstone	100	0.56	
30	3	aleurolite	60	0.33	
26	4	aleurolite	50	0.28	
23	3	sandstone	90	0.50	
18	5	aleurolite	50	0.28	
15	3	sandstone	100	0.56	
10	5	aleurolite	50	0.28	
9	1	*coal*	15	0.08	productive formation H = -960 m
6	3	aleurolite	60	0.33	
0	6	sandstone	90	0.50	

of equivalent materials and recipes were established: 1 - reproduction of coal based on DEG-1 resin (the condensation product of epichlorohydrin with diethylene glycol, contains at least 26% of epoxy groups), 2 - reproduction of sandstones based on ED-20 resin (oligomeric product based on diphenylolpropane diglycidyl ether, contains 20% of epoxy groups), 3 - reproduction of argillite and aleurolites based on ED-20 resin, providing reproduction of physical and mechanical characteristics of the massif (Table 1), presented in table 2.

Table 2- Characteristics of the EM main types and binder formulations.

Parameter / Name	Layer thickness (cm)	Strength (Mpa)	EM type
Coal	1.5- 4	0.08	DEG-1 Cs=0.7
Sandstone	2-12	0.39-0.68	ED-20 Cs=0.72-0.81
Argillite	1-2	0.22	ED-20 Cs=0.64
Aleurolite	2-12	0.22-0.36	ED-20 Cs=0.64-0.7

*Cs – resin content in EM

The physical model is manufactured on a stand with a simulated area of 5000x1100x200 mm, the scheme of which is shown in figure 1.

The physical model reproduced the region of massif from -951 m to -841 m. In this case, geomechanical processes depend on gravitational forces, the vertical components of which are determined by the weight of the overlying mass of the massif, and the horizontal ones - by passive lateral repulsion (according to Dinnik), which is provided by rigid stand side walls (Figure 1).

The loading of the model provides reproduction of the overlying mass of the massif on the simulated area, using a loading device with a pneumatic cushion.

The parameters of vertical and horizontal displacements were determined using reference marks of the "quadrant" type, installed on the front surface of models No. 1, 2, 3 on various horizons. Displacement parameters were determined using a Hasselblad H5D-200MS high-resolution photographic recorder with an accuracy of 15–33 mm on location. Low error rates were achieved due to the high-resolution shooting of 200 or 50 megapixels.

3. Results and Discussion

In model No. 1, the collapse zone was formed due to mining only the upper productive layer (H = -930 m). In this case, a clear dynamic nature of the collapse is observed - rock bump (Figure 2). This is confirmed by a similar characteristic of these layers in different mines of the Vorkuta coal basin. Such mining technique is unsafe.

In model No. 2, the lower coal seam was mined as protective to the upper one. Such mining technique reduces the rock-bump hazard of the layer, unloading it with cracks from the collapse of the roof of the lower
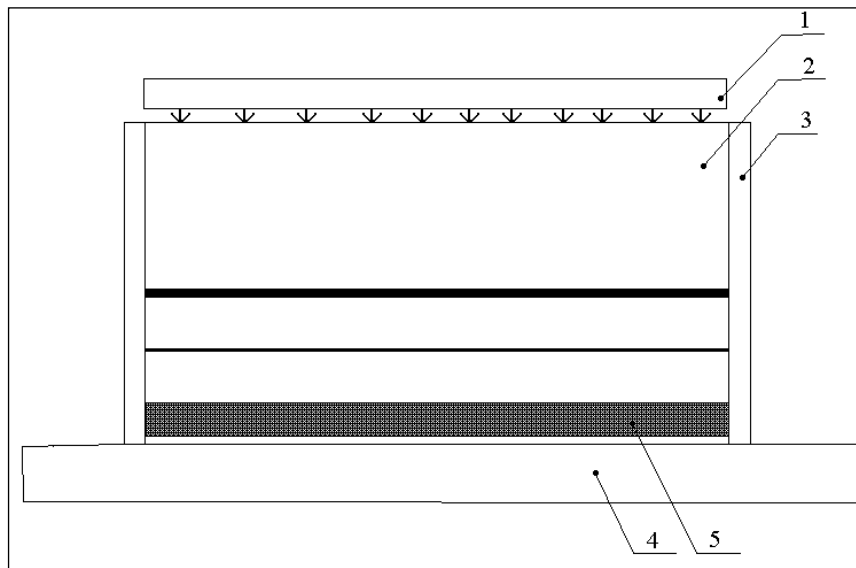

Figure 1- Schematic diagram of the stand (1 - loading device; 2 – model; 3 - side wall; 4 – stand base, 5 - sliding formwork).
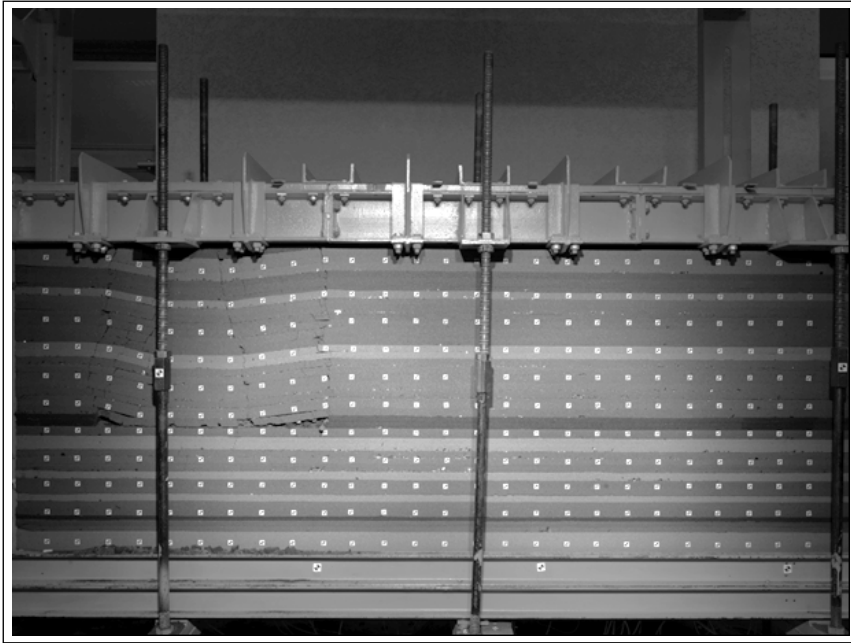
Figure 2- Formation of the collapse zone in model no. 1.

layer. However, in this case, the flow of methane, into the bottom of the upper coal seam from the interlayer thickness and the emerging zone of collapse of the lower coal seam in the roof of the upper coal seam, increases (Figure 3).

In model no. 3, the impact on the collapse zone of the complex structure of the roof of the upper coal seam was estimated, while maintaining the ascending order of mining. This worsens the geomechanical state of mining of the upper coal seam (Figure 4).

The results of the distribution of vertical displacements of the rock layers at different horizons are presented in figures 5-9.
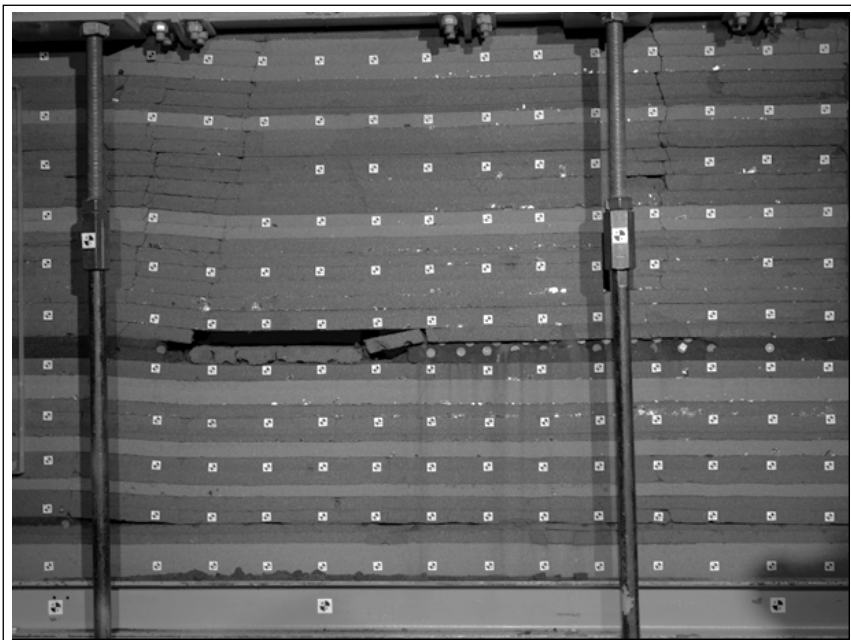

Figure 3- Formation of the collapse zone in model no. 2.
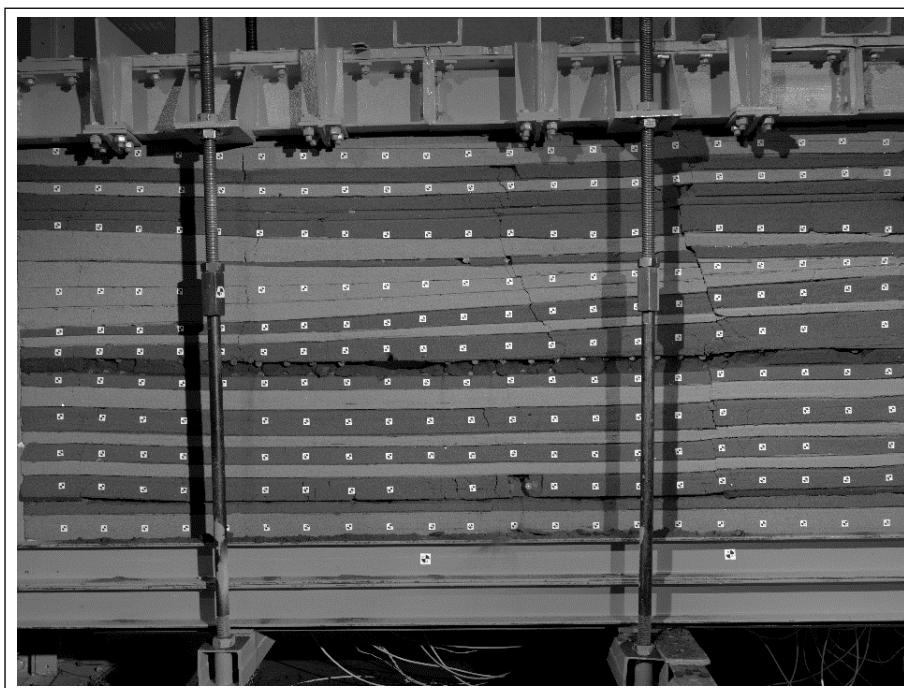
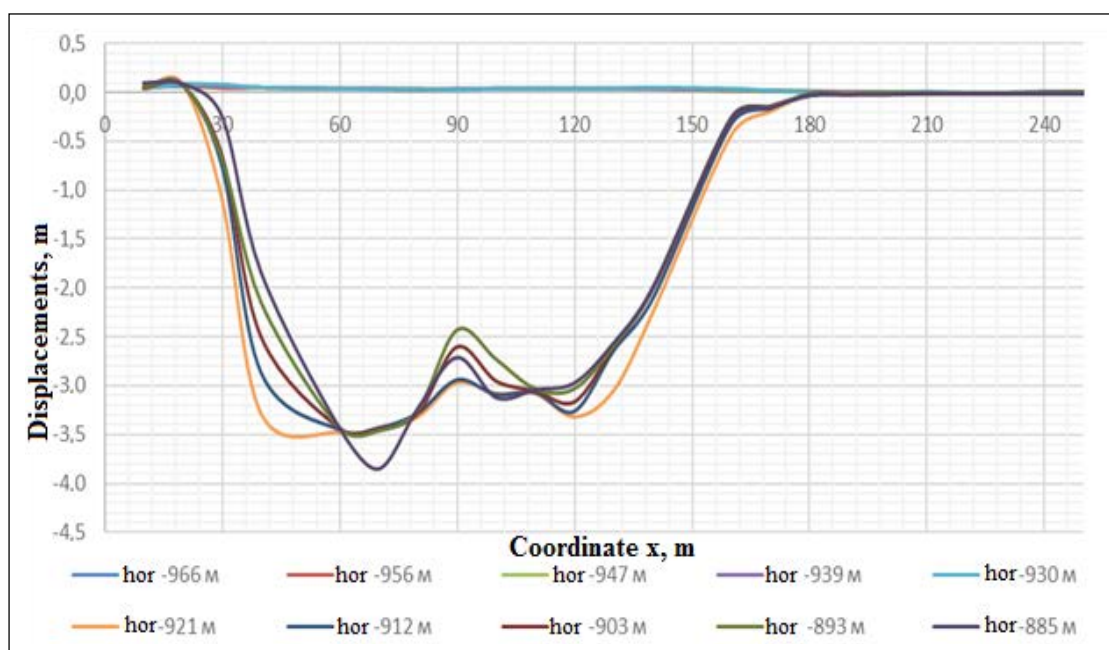Figure 4- Formation of the collapse zone in model no. 3.

Figure 5- Vertical displacements in model No. 1 on horizons from -859 m to -969 m with a distance of the stope of 155 m.
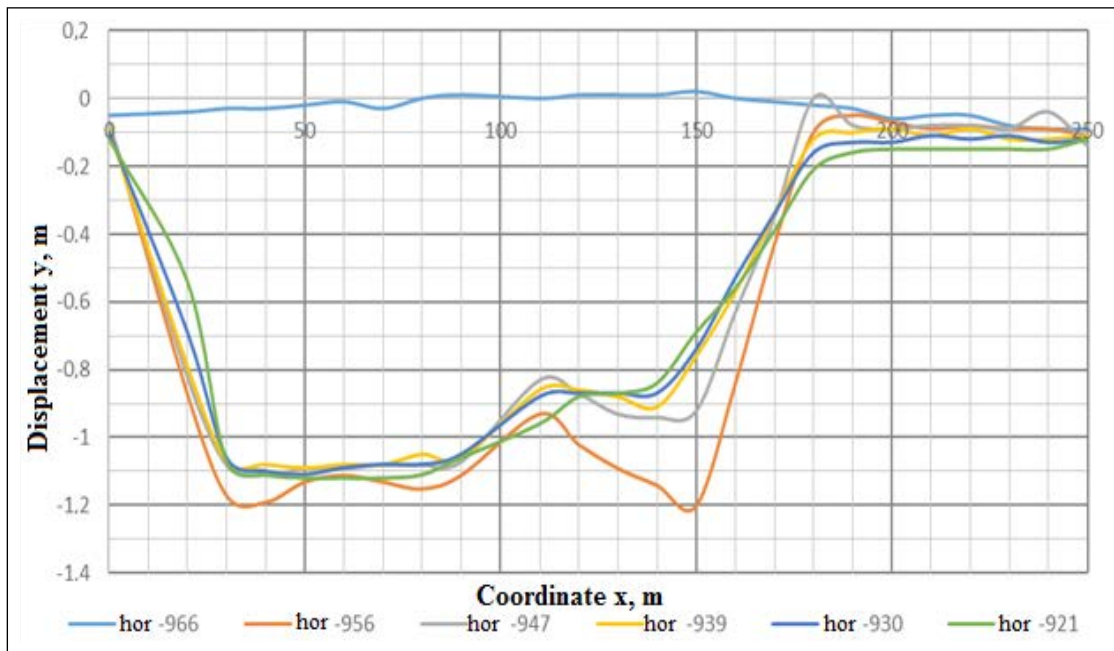
Figure 6- Vertical displacements in model no. 2, when mining the lower industrial formation at horizons from -921 m to -966 m with a span of 130 m.
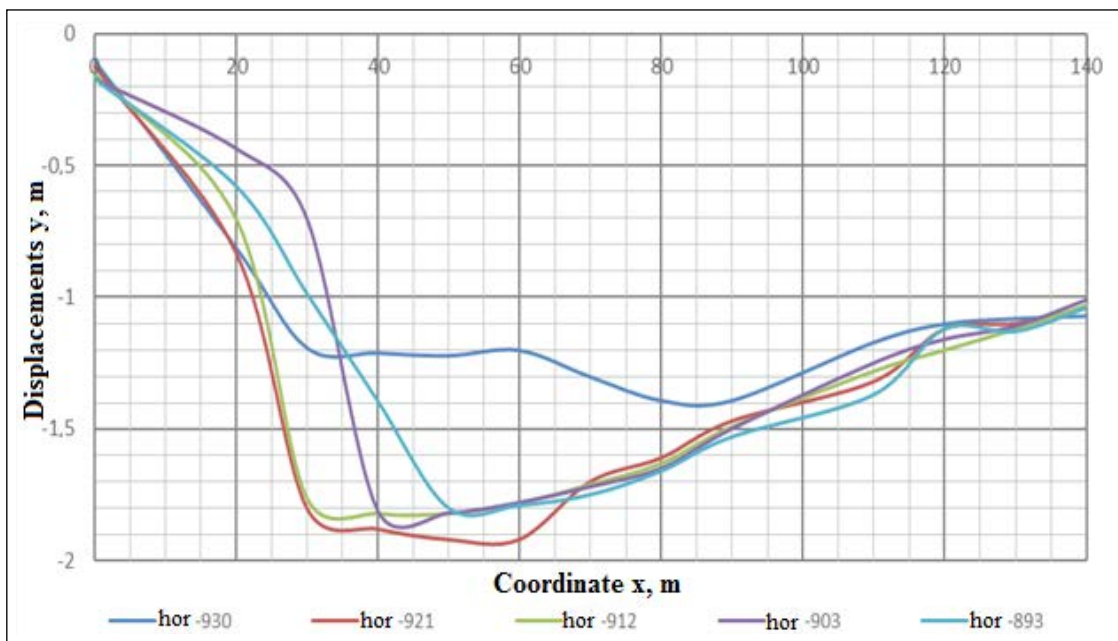

Figure 7- Vertical displacements in model no. 2, when mining the upper industrial formation at horizons from -893 m to -950 m with a span of 50 m.
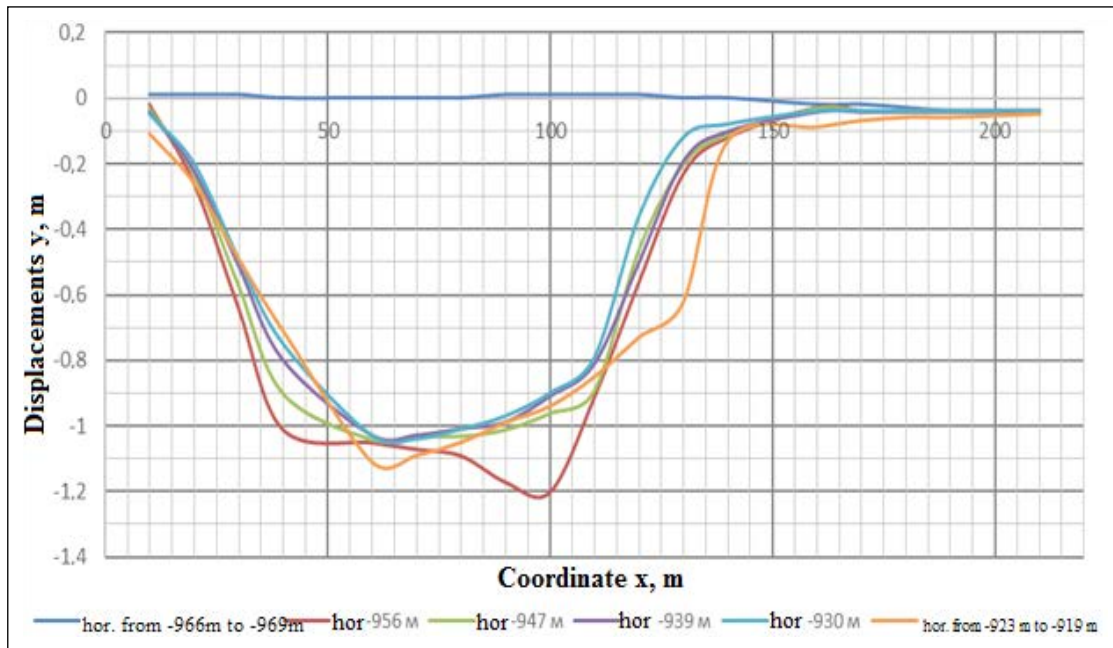
Figure 8- Vertical displacements at different horizons in model no. 3 in the horizon range from -969 to -919 m with a span of 160 m.
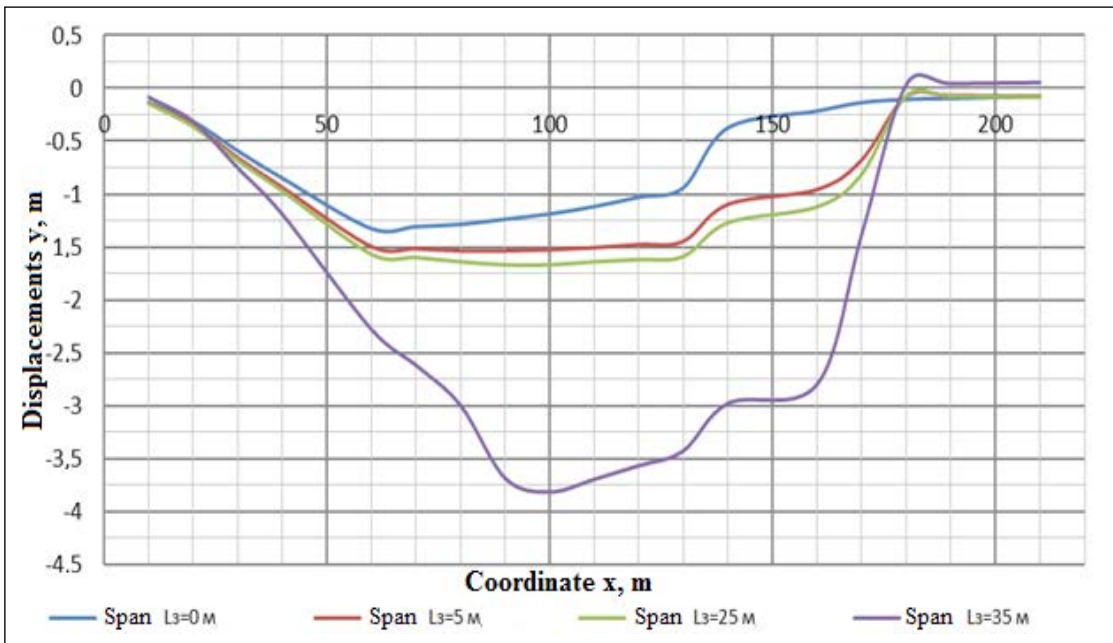

Figure 9- Vertical displacements in model No. 3 at the level of the immediate roof of the upper coal seam when wedging out a layer of sandstone in the rocks of the main roof at horizons -923 m -919 m.

Figures 5-8 show the displacements of different horizons during the collapse according to the reference marks on the surface. Displacements were recorded in each horizon above the developed layers, and their magnitude shows that the rock layers move together almost without decompaction. This means that these horizons are unstable and destroyed in reality. Sharp edges of the graphs reflect the roof caving behind the stope with a small step (10-30 m), and almost complete elimination of the voids of the goaf. Therefore, methane from there, except for small leaks, all goes to the bottom during the collapse.

Figure 9 shows the first roof caving, when mining the upper coal seam; initial displacements were formed after the lower seam was mined. The step size is 35 m. The collapse pattern corresponds to that in previous figures (sharp edges - without hanging the roof, the value corresponds to the thickness of the seam - no decompaction) was evident:

- When mining only the upper coal seam, the zone of the first collapse is 155 m.

- When mining sequentially, first the lower coal seam, then the upper coal seam, without considering the pinching-out of rocks, the collapse zone is 130 m.

- When mining sequentially, first the lower coal seam, then the upper coal seam, considering the pinching-out of rocks, the zone of collapse is 160 m.

In all models, the main width of the collapse zone is formed due to the mining of the upper coal seam and follows the stope. This is due to the thickness of the upper coal seam (4 m). A slightly smaller zone of collapse in model No. 2 shows the effectiveness of mining the lower coal seam as a protective one:

- The largest zone of collapse is observed when the rocks are pinching out. The nature of cracking and the width of cracks in model No. 3 indicates a positive effect of pinching on the expansion of the collapse zone. This is due to the large depth of mining, when even minor irregularities and bedding angles can lead to a change in the nature of the loading, from compression to tension and bending, reducing the strength and stability of rocks.

- The zone of collapse covers all simulated horizons and practically does not change along the mining width. The angle α showing the rock cavity is almost 90º. Without additional studies covering the simulated zone of not less than 100 layer thicknesses, it is not possible to predict the zone of influence.

4. Conclusions

The calculated collapse zone is approximately 30% larger than the project. This is due to the imperfection of computational techniques that do not consider a number of factors affecting the methane release from guiding beds. These factors include – the layers mining order, increased depth of mining, and the presence of violations in the roof of the developed seam.

The simulation confirmed the correctness of the design solution for mining the lower coal seam as a protective one. The collapse zone in this case has decreased. However, studies have shown the need to adjust the project for a larger methane yield. To clarify the characteristics of the collapse zone, it is necessary to conduct additional studies on a large scale modeling. The results of further research can be used to adjust the method for predicting methane inflow, into the stope from guiding beds; use of advance and preliminary degassing; the speed of the face movement and the required air volume.

References

Akıska, S., Akıska, E. 2018. An ore adit planning with the help of three dimensional ore body modeling: A case study from Çulfa Çukuru Pb-Zn-Cu-Ag deposit. Bulletin of the Mineral Research and Exploration 157, 201-217. DOI: 10.19111/bulletinofmre.372510.

Andreev, R.E., Gridina, E.B. 2016. A study of gas-dynamic processes in a charge chamber during the explosion of blasthole charges of various designs. Research Journal of Pharmaceutical, Biological and Chemical Sciences 7 (3), 2383-2392.

Bai, Q., Tu, S., Wang, F., Zhang, C. 2017. Field and numerical investigations of gateroad system failure induced by hard roofs in a longwall top coal caving face. International Journal of Coal Geology 173, 176-199.

Cherkai, Z.N., Gridina, E.B. 2017. Technological problems and fundamental principles of methods of engineering-geocryological exploration during construction and exploitation of wells in permafrost rock mass. Journal of Mining Institute 223, 82-85.

Gao, F., Stead, D., Coggan, J. 2014. Evaluation of coal longwall caving characteristics using an innovative UDEC Trigon approach. Computers and Geotechnics 55, 448-460.

Gao, F., Kang, H., Lou, J., Li, J., Wang, X. 2019. Evolution of local mine stiffness with mining process: Insight from physical and numerical modeling. Rock Mechanics and Rock Engineering 52(10), 3947-3958.

Gridina, E.B., Andreev, R.E. 2016. Principles of providing safety, comprehensive analysis of the injury risk and the targeted impact on the traumatic factors as the instruments of increasing the efficiency of integrated safety management systems at mining enterprises of the Russian Federation. Research Journal of Pharmaceutical, Biological and Chemical Sciences 7 (3), 2641-2650.

Grigoriev, B.S., Eliseev, A.A., Pogarskaya, T.A., Toropov, E.E. 2019. Mathematical modeling of rock crushing and multiphase flow of drilling fluid in well drilling. Journal of Mining Institute 235, 16-23.

Kang, H., Lou, J., Gao, F., Yang, J., Li, J. 2018. A physical and numerical investigation of sudden massive roof collapse during longwall coal retreat mining. International Journal of Coal Geology 188, 25-36.

Kanık, M., Gürocak, Z., Alemdağ, S. 2015. A comparison of support systems obtained from the RMR89 and RMR14 by numerical analyses: Macka Tunnel project, NE Turkey. Journal of African Earth Sciences 109, 224-238.

Kaya, A., Bulut, F., Sayın, A. 2011. Analysis of support requirements for a tunnel portal in weak rock: A case study from Turkey. Scientific Research and Essays 6(31), 6566-6583.

Kazanin, O.I., Sidorenko, A.A. 2017a. Interaction between gas dynamic and geomechanical processes in coal mines. ARPN Journal of Engineering and Applied Sciences, 12 (5), 1458-1462.

Kazanin, O.I., Sidorenko, A.A. 2017b. The best available technologies for horizon mining of flat-lying gaseous coal seams: Prospects for development in Russian mines. ARPN Journal of Engineering and Applied Sciences 12 (1), 227-23

Kazanin, O.I., Sidorenko, A.A., Vinogradov, E.A. 2017. Substantiation of the technological schemes of intensive development of gas-bearing coal beds. ARPN Journal of Engineering and Applied Sciences 12 (7), 2259-2264.

Li, N., Wang, E., Ge, M., Liu, J. 2015. The fracture mechanism and acoustic emission analysis of hard roof: a physical modeling study. Arabian Journal of Geosciences 8(4), 1895-1902.

Pan, W., Nie, X., Li, X. (2019). Effect of premining on hard roof distress behavior: a case study. Rock Mechanics and Rock Engineering 52(6), 1871-1885.

Sidorenko, A.A., Sishchuk, J.M. 2016. Stability of undermining seam panel entries at retreating longwall multiple mining. Research Journal of Pharmaceutical, Biological and Chemical Sciences 7 (2), 927-935.

Sidorenko, A.A., Sirenko, Yu.G., Sidorenko, S.A. 2018. Influence of face advance rate on geomechanical and gas-dynamic processes in longwalls in gassy mines. Eurasian Mining 1, 3-8.

Sidorenko, A.A., Ivanov V.V., Sidorenko S.A. 2019. Numerical simulation of rock massif stress state at normal fault at underground longwall coal mining. International Journal of Civil Engineering and Technology (IJCIET) 10, 844–851.

Sidorov, D.V., Potapchuk, M.I., Sidlyar, A.V. 2018. Forecasting rock burst hazard of tectonically disturbed ore massif at the deep horizons of Nikolaevskoe polymetallic deposit. Journal of Mining Institute 234, 604-611.

Wang, G., Wu, M., Wang, R., Xu, H., Song, X. 2017. Height of the mining-induced fractured zone above a coal face. Engineering Geology 216, 140-152.

Wang, F., Jiang, B., Chen, S., Ren, M. 2019a. Surface collapse control under thick unconsolidated layers by backfilling strip mining in coal mines. International Journal of Rock Mechanics and Mining Sciences 113, 268-277.

Wang, H., Shi, R., Lu, C., Jiang, Y., Deng, D., Zhang, D. 2019b. Investigation of sudden faults instability induced by coal mining. Safety Science 115, 256-264.